ELSEVIER

Chemical Engineering Journal 80 (2000) 13–22

Chemical Engineering Journal

www.elsevier.com/locate/cej

Aggregate structures formed via a bridging flocculation mechanism

Simon Biggs [a,*], Michael Habgood [a], Graeme J. Jameson [b], Yao-de Yan [b]

[a] *Department of Chemistry, Centre for Multiphase Processes, The University of Newcastle, University Drive, Callaghan, NSW 2308, Australia*
[b] *Department of Chemical Engineering, Centre for Multiphase Processes, The University of Newcastle, University Drive, Callaghan, NSW 2308, Australia*

Abstract

A high molecular weight cationic polyelectrolyte has been used to flocculate a colloidal dispersion of anionic polystyrene latex particles. The polymer used had a high charge density and the flocculation occurred at a solution pH where both the polymer and the particles were fully charged. Under these conditions, flocculation is expected to occur through a bridging flocculation mechanism. Low angle laser light scattering has been used to follow the flocculation process as a function of time; parameters of interest were the aggregate sizes, size distributions, and aggregate mass fractal dimensions. The light scattering measurements showed that the flocs formed had a mass fractal character. All the systems examined here were overdosed with respect to the optimum flocculation concentration of polymer. Under these conditions, decreasing the polymer concentration was seen to result in an increased flocculation efficiency. A secondary growth process was also observed whereby initially formed fractal aggregates can subsequently aggregate again. These larger aggregates are also expected to be mass fractals although this cannot be determined from the light scattering measurements due to the superposition of Fraunhofer diffraction effects. This type of fractal-in-fractal character is unusual.

Keywords: Bridging flocculation; High molecular weight polymer; Mass fractal dimension; Low angle laser light scattering; Aggregate structure

1. Introduction

Bridging flocculation continues to be a widely used technique for the removal of solid particles from an aqueous dispersion [1]. It has application in many important industries including wastewater treatment and paper manufacture. Ruehrwein and Ward first proposed the basic principle of bridging flocculation in 1952 [2]. In their paper, they presented a model where a single polymer chain was bridging between two or more particles. The basics of this model have been subsequently refined, but the main points are unchanged; the loops and tails of the adsorbed polymer structure on one particle protrude into solution and can attach to a second particle. La Mer and co-workers provided further insights of the bridging flocculation process in a series of classic papers [3–5]. Smellie and La Mer [4] postulated that the surface coverage of adsorbed polymer was a fundamental parameter controlling the probability of bridging. Subsequently, Healy and La Mer [5] introduced the concept of 'half surface coverage' as being the optimum condition for flocculation to occur.

Control of the aggregate structures formed during a bridging flocculation process is not easy [6]. Parameters such as polymer chemistry, polymer charge, particle surface charge, polymer dosage, and the mixing regime will be important. The primary factor to control is the structure of the adsorbed polymer layer; the conformation should be of a loops and tails type. There should also be some particles with available free surface to facilitate the bridging. In an actual flocculation process the development of an adsorbed polymer structure occurs in a dynamic environment. Gregory [7] has introduced the concept of non-equilibrium flocculation to explain such processes. In this model, flocculation can only occur when a particle with free surface encounters a particle carrying some 'active' polymer; 'active' polymer is a polymer that has only recently adsorbed to the surface and has some long loops and tails. Obviously, the active state of a polymer is a transient condition. The optimum structure will only have a certain lifetime. This lifetime will be controlled by the relative surface area to polymer concentration ratio, the size of the polymer, the adsorption energy of the polymer segments to the solid surface, and the collision frequency between particles. A higher concentration of particles will lead to a higher collision frequency and hence an increased probability of finding the polymer in an active state. Of course, an increase in collision frequency can also be attained from an increase in agitation during mixing.

In real applications it is normal to introduce a polymer flocculant to the colloidal dispersion of interest in a turbulent mixing situation; in minerals processing for example this occurs in a thickener. Any polymer coil in solution will have

* Corresponding author. Tel.: +61-2-49215481; fax: +61-2-49215472.
E-mail address: chsrb@cc.newcastle.edu.au (S. Biggs).

1383-5866/00/$ – see front matter
PII: S1383-5866(00)00072-1

definite dimensions [8]. These dimensions are controlled by the solvent affinity for the polymer chain segments. A high solvent affinity will lead to an expanded coil conformation; a poor affinity will cause coil collapse. At the initial moment of adsorption to the surface, the coil will retain its solution conformation [9]. The polymer will then attempt to relax towards the surface. The amount of relaxation is controlled both by the adsorption affinity of the segments for the surface and the solvency of the chain. In a good solvent the chain will want to maximise its contacts with the solvent and a loops and tails conformation will be favoured. The rate of polymer adsorption will also play an important role; steric crowding of chains on the surface will tend to favour an extended conformation away from the interface [10]. The adsorption step and the structural developments will occur simultaneously with particle mixing and collision in a dynamic mixed system. As a result, deciphering the relative importance of each of these processes is extremely difficult. Adachi et al. [11] noted that, as a result of these difficulties, very little work on the dynamic aspects of bridging flocculation has been reported.

Previous research on the action of polymer flocculants is extensive [12–14]. However, very little of this literature has examined the aggregate structures formed during the flocculation process. Ultimately, to gain good control of any flocculation process a thorough knowledge of the resultant aggregate structures that are formed is vital. Some evidence of the structures that can form in a bridging process has been obtained using transmission electron microscopy [15,16]. The results indicated a structure that consisted of large filamentous matrices of polymer holding small inorganic particles together in an aggregate. Although these images are useful, this approach has some inherent difficulties. To obtain an image it is necessary to remove the aggregate from the solvent and to dry it. This can lead to structural change. Also, the image is a two-dimensional projection of the three-dimensional reality.

In a recent series of papers, Stoll and Buffle [17,18] have reported the results of simple off-lattice simulations of bridging aggregation. In these simulations, three-dimensional aggregate structures were generated. The primary variables of control were the polymer to particle concentration ratio and the size and shape of the polymer chain (i.e. coil or rod). Geometrical analyses of the floc structures generated indicated that, for a random polymer coil, the mass fractal dimension of an aggregate is between 1.9 and 2.1; these fractal numbers are independent of the polymer/particle ratio.

In the present study, we have been using low angle laser light scattering (LALLS) to obtain information about the size and structural compactness of aggregates formed when a model anionic polystyrene latex sample is flocculated using high molecular weight cationic polymers. Although this is the situation typical in an industrial bridging flocculation system, no attempt was made here to accurately mimic any real set of conditions. The primary concern of this work is whether or not LALLS can be used to gain any useful information about large aggregates with relatively open structures. To form such structures a bridging flocculation route was chosen.

Recently, fractal analysis techniques have been applied to the characterisation of aggregate structures in colloidal systems using light scattering [19,20]. The results of these studies give an indication of the structure of an aggregate and its density. Sedimentation effects often complicate studies of aggregation processes associated with polymer bridging using light scattering. Sedimentation is a major problem due to the size of the aggregates that form which are often more than 100 μm in diameter. The use of polystyrene latex particles as a model colloidal system allows light scattering experiments to be performed over extended time periods without the associated problems of settling due to the almost density matching of the particles with the water.

2. Background theory

Aggregates of colloidal particles have been shown to be mass fractal in nature [19,20]. Any fractal object is said to be 'self-similar' which simply means that it appears to have the same structure regardless of the length scale of the observation. For a three-dimensional aggregate in standard Euclidean space the mass fractal dimension, d_F, is a convenient tool to characterise the density of the aggregate. Essentially, it describes the space-filling capacity of the aggregate in question. For any mass fractal aggregate, the mass, $m(R)$, of the aggregate is directly proportional to its radius, R, raised to a power equal to d_F, according to

$$m(R) \propto R^{d_F} \tag{1}$$

Furthermore, the fractal dimension can be used to characterise changes in aggregate mass density, $\rho(R)$, through,

$$\rho(R) \propto R^{d_F-3} \tag{2}$$

In both cases, $1<d_F<3$ and is not limited to integer values unlike traditional mass–radius relationships.

Determination of the fractal dimension is usually achieved from radiation scattering experiments. For colloidal objects with dimensions of between 10 and 500 nm LALLS has been shown to be applicable for aggregate structural analysis [21]. In any light scattering study, the scattered intensity as a function of the magnitude of the scattering wave vector, q, is measured, where,

$$q = \frac{4\pi n_0}{\lambda_0} \sin(\theta/2) \tag{3}$$

In this equation, n_0 is the refractive index of the dispersion medium, θ is the scattering angle and λ_0 is the incident light wavelength in vacuo. q has the units of l/length and essentially $1/q$ gives the spatial resolution of a scattering experiment. For an individual colloid particle of radius r_0 we can see that if $r_0 \gg 1/q$ then we will observe interference

patterns from within the primary particles. In contrast, for $r_0 \ll 1/q$ the scattering interference pattern observed will come from different particles. Thus, by observing a range of q it is possible to probe structural correlations at increasing separations within the aggregate.

It has been shown that for a mass fractal aggregate which satisfies the conditions for the Rayleigh–Gans–Debye (RGD) regime, its scattered intensity $I(q)$ is described by the following equation [21],

$$I(q) = k\,P(q)\,S(q) \tag{4}$$

where k is a scattering constant relating to the measuring geometry and the optical properties of a primary particle, $P(q)$ is the primary particle form factor and $S(q)$ is the interparticle structure factor. $S(q)$ describes the correlations between individual particles in an aggregate, assuming that there are no correlations between the aggregates. When $qr_0 \gg 1$, $S(q) \sim 1$ and the observed scattering essentially comes from the individual primary particles only. However, when $1/R \ll q \ll 1/r_0$ we see that $P(q) \sim 1$ and $S(q)$ reduces to

$$S(q) \propto q^{-d_F} \tag{5}$$

and, if $R \gg r_0$ then we can write,

$$I(q) \propto S(q) \propto q^{-d_F} \tag{6}$$

Thus, by recording the scattered intensity as a function of the magnitude of the scattering wave vector for an aggregate we are able to determine the fractal dimension from the slope of a simple log–log plot in the appropriate q range.

3. Experiment

3.1. Materials

All water used here was of Millipore Milli-Q grade. Potassium nitrate (KNO_3), nitric acid (HNO_3) and potassium hydroxide (KOH) were analytical grade reagents (BDH Chemicals) and were used as supplied. All glassware was rigorously cleaned prior to use.

3.2. Latex particles and polymers

The polystyrene latex particles were synthesised according to the method of Goodwin et al. [22] using ammonium persulphate as the initiator. The resultant particles were with an average particle radius of 165 nm and with a polydispersity of <3%. Electrophoresis measurements indicated that the particles were fully charged at any pH > 6.

The polymer used here was a quaternary ammonium based derivative of polyacrylamide (SNF Floeger) and had a molecular weight of 16×10^6 and a manufacturer's quoted nominal cationic charge density of 100%. The polymer was used as supplied without further purification.

All the measurements performed here were carried out at pH 6 in 10^{-4} M KNO_3.

3.3. Dispersion stability measurements

The stability of colloidal dispersions of the latex sample was examined visually as a function of polymer/particle concentration ratio. Immediately after preparation, the samples were vigorously mixed for 2 min and then allowed to stand in sealed tubes for a total of 24 h. After this time the state of the tubes was assessed in terms of the amount of settling and the apparent size and structure of any aggregated material. Each of these measures was non-quantitative.

3.4. Light scattering studies (LALLS)

Stable latex dispersions were initially prepared in a beaker in 10 cm^3 batches at a concentration of 0.05% (w/w). These dispersions were then vigorously stirred using a magnetic stirrer. Each sample was stirred at the same speed using the same stirring bead to ensure uniform conditions. A small aliquot of the chosen polymer (<1 cm^3) was then added to the stirred dispersion at some concentration such that a desired final polymer concentration could be achieved. After stirring for 60 s, the sample was removed from the stirrer and immediately diluted using the background electrolyte solution to a concentration suitable for light scattering measurements to be taken. In all cases, the dilution factor was constant.

The sample was then gravity fed into the scattering cell and the aggregation process monitored under perikinetic conditions as a function of time by means of a low angle laser light scattering device (Malvern Mastersizer E, Malvern Instruments, UK). This device monitors simultaneously the intensity of light scattered at a number of angles from 0 to 46°. These data are used to calculate the particle or aggregate sizes for any object of up to 880 μm. It should be noted that there is some uncertainty in the absolute aggregate size information obtained from the Mastersizer due to the fact that the commercial data analysis program used treats any scattering object as a solid sphere and not a porous object. However, the observed trend in the change of particle size with time for an aggregating system will still be correct.

Fractal information, as a function of time, was calculated by plotting the intensity of light scattered as a function of the magnitude of the scattering wave vector on a double logarithmic scale, i.e. $\log I(q)$ versus $\log q$ plots.

4. Results and discussion

The major aim of this work was to determine if LALLS techniques could be applied to determine structural information for large porous aggregates. To generate such aggregates, it was decided to use bridging flocculation of primary latex particles. No attempts were made to accurately mimic

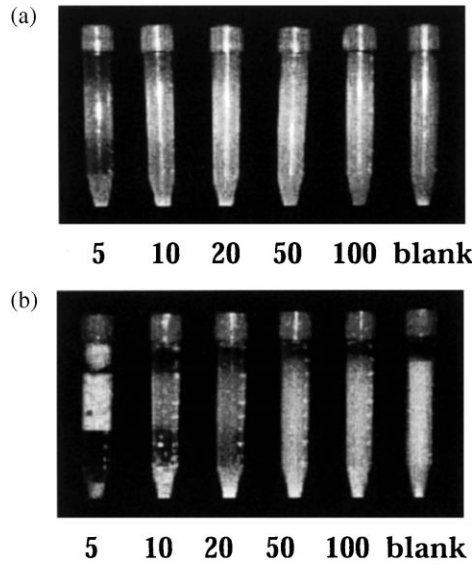

Fig. 1. The effects of added polymer flocculant on the stability of an aqueous anionic colloidal polystyrene latex dispersion. The photographic images presented are for a range of polymer concentrations at two initial particle concentrations: (a) 0.05% (w/w) and, (b) 0.2% (w/w). Other conditions: pH 6; $(KNO_3)=10^{-4}$ M; $T=25^{\circ}C$.

'real' conditions of mixing or dosage, as would be applied in an industrial application. Rather, we used flocculant conditions for which the system was slightly overdosed. As we shall show below, this did not prevent the flocculation leading to large aggregates, but it did slow down the growth of the aggregates sufficiently to allow us to more accurately monitor the structural development as the size increased.

The effects of the added polymer on the stability of latex dispersions are illustrated in Fig. 1; the two series of tubes shown are for two particle concentrations (0.05 and 0.2% w/w) and a range of polymer concentrations (0–100 ppm). At the lower of the two particle concentrations none of the polymer concentrations used can be considered as being particularly efficient at flocculating the system. This was not the case at the higher particle concentration where 5 ppm polymer was seen to be efficient at flocculating the dispersion. For both of the particle concentrations a decrease in the efficiency was seen as the polymer concentration was increased. Closer examination of the results for the lower particle concentration indicated that the tube at 5 ppm polymer also had a lower turbidity than the higher polymer concentrations. This indicates that optimum flocculation will be achieved at an even lower polymer concentration and that the system is slightly overdosed. It should be noted that the photos presented here were taken after 24 h. Leaving these settling tubes for a much longer time period, of over 4 weeks, resulted in significant sedimentation in all the tubes with added polymer. The amount of sediment formed decreased as the polymer concentration increased. The blank samples were stable over the time period. Due to the near density matching of latex particles in water, open porous flocs can take long time periods to settle even when they are quite large. Therefore, we are confident that some flocculation will occur at all the polymer and particle concentrations examined although it may not be obvious from these photographs. The flocculation will be confirmed below with LALLS data.

Healy and La Mer [5] argued that the optimum condition for flocculation occurs at the 'half-surface coverage' point. Below this point, each particle has a large amount of free surface area with relatively few adsorbed polymer chains. At very low surface coverage, a collision between particles may occur between bare areas and so bridging may not result. As the coverage increases towards 50%, a collision is increasingly likely to result in polymer bridging between the particles. Above a surface coverage of 50%, increasing coverage will result in a decreased likelihood of bridging since collisions between surfaces will tend to lead to polymer overlap and steric repulsion. Furthermore, flocculation is a dynamic process dependent on a number of factors. Included in these factors are the particle collision rate, polymer adsorption rate and the relaxation rate of polymer at the solid–liquid interface. In a real system, after mixing of the polymer and particles, we would expect the surface coverage to increase as a function of time. The rate of this increase will depend on the relative magnitudes of the above three rates. This has important consequences if optimum flocculation is to be achieved. In effect, there will always be some time window at which the surface coverage will be close to the optimal value of 50%. The closer we are to the optimum polymer dosage for any given system (under constant temperature and shear conditions), the longer this time period will be. Thus, for overdosed systems if the adsorption and relaxation rates are not rapid when compared to the particle collision rates we may expect flocculation to occur. This point will be discussed in more detail below with reference to Figs. 8 and 9.

A representative series of data for the aggregate size distributions as a function of time, at one polymer concentration (20 ppm) and at a latex concentration of 0.05% (w/w) prior to dilution, are given in Fig. 2. The general features of these data are typical for all the samples tested here at all polymer concentrations. Three size regions are immediately apparent in the data: (i) 0.1–1 μm, the 'primary particle' region; (ii) 1–100 μm, the 'primary aggregate' region; and (iii) >100 μm, the 'secondary aggregate' region. In general, the initially measured data, at 2 min, consisted mostly of the primary aggregates although some of the primary particles were often still present. Over the course of 30 min in the scattering cell, under no agitation, the secondary aggregate peak was seen to grow, whilst the other two peaks were seen to decrease. The relative extent of these changes depended strongly upon the polymer concentration.

The abundance of the mid-sized flocs immediately after stopping the agitation and their subsequent growth to very large sizes under perikinetic conditions imply that the shear forces involved during the mixing stage were sufficient to limit floc growth. Immediately after the shear field is removed, the aggregates formed in the mixing stage diffuse together and grow to the larger sizes observed.

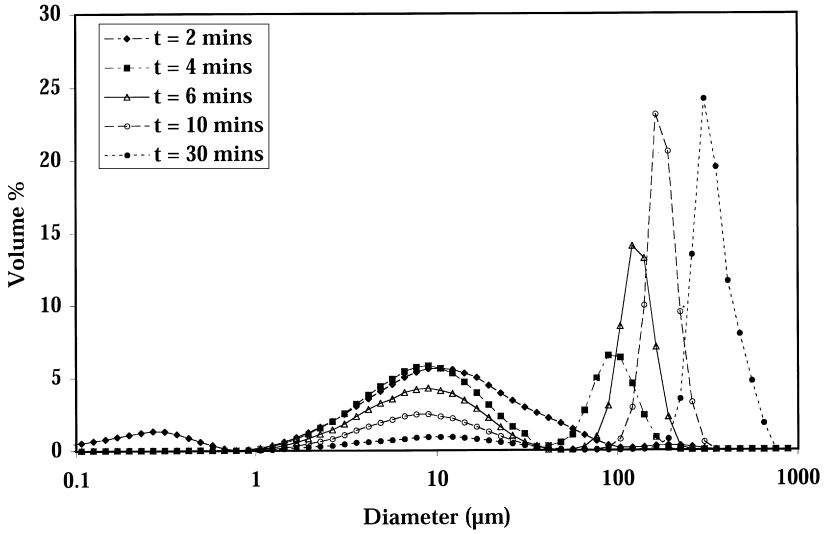

Fig. 2. Data of the measured aggregate size distributions collected at five different times after the sample was initially mixed. The initial system conditions used (prior to dilution): polymer flocculant concentration=20 ppm; particle concentration=0.05%; pH 6; $(KNO_3)=10^{-4}$ M; $T=25^{\circ}C$.

Further evidence for the two stage growth process is found when we consider the $\log I(q)$ versus $\log q$ plots. The log–log plots for the intensity data corresponding to the data in Fig. 2 are given in Fig. 3. The most striking feature of these data is the two step nature of the plots at longer time scales.

Let us consider initially the data at a time of $t=2$ min. In this plot, as described above, $1/q$ represents a characteristic length scale. At very low q, the length scale probed is larger than any aggregate present and we simply probe the mean mass of the aggregates. This is seen as a flat portion of the data. At large q ($\log q > -2$) (inaccessible here due to equipment limitations), the length scale probed would be smaller than the size of the primary particles. In such a case, there would be no contribution from $S(q)$ and we would only probe the primary particles present. At intermediate q values (accessible here) we are able to probe the structure of the aggregates. This data set, at $t=2$ min, shows an essentially classical fractal result. The linear slope of the data at $-3 < \log q < -2$ will give the mass fractal dimension of the primary aggregates. In this case, the mass fractal dimension is $d_F=1.59$; this indicates a highly open structure [20]. Such a structure would be consistent with a diffusion controlled mechanism.

The two step character in the $\log I(q)$ versus $\log q$ data seen at the longer times is unusual. The linear region at the higher q values ($-3 < \log q < -2$) is apparently conserved

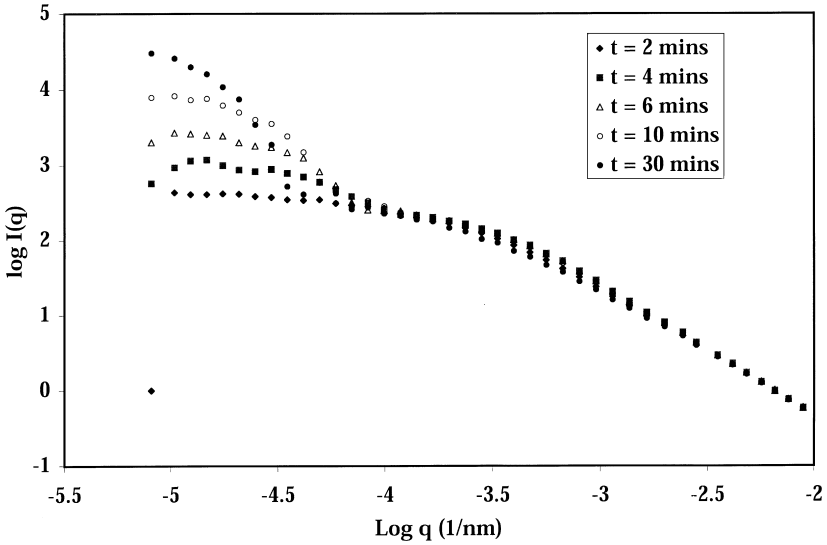

Fig. 3. The measured intensity of scattered light as a function of q collected at five different times after the sample was initially mixed. The data are presented on a double logarithmic scale. The initial system conditions used (prior to dilution): polymer flocculant concentration=20 ppm; particle concentration=0.05% (w/w); pH 6; $(KNO_3)=10^{-4}$ M; $T=25^{\circ}C$.

throughout the experiment. This region corresponds to the fractal behaviour of the primary aggregates. At smaller values of q, the secondary rise in the data corresponds to scattering from the larger secondary aggregates.

Before discussing these data further it is necessary to return to the data presented in Fig. 2 and our postulate for a two-stage flocculation mechanism. Evidence that the secondary aggregates are formed from flocculation of the primary aggregates can also be seen in Fig. 3. The $\log I(q)$ versus $\log q(-4 < \log q < -2)$ data indicate clearly that the scattered intensity from the primary aggregates does not alter with time. This is despite the fact that the size distribution data show clearly that these aggregates are 'disappearing' with time. The only way that this can be rationalised is that they are still present in the secondary aggregates. This type of aggregate-in-aggregate structure is shown schematically in Fig. 4. To maintain a constant scattering intensity as a function of time the total number of primary aggregates must be conserved during the aggregation process.

The form of the data sets seen in Fig. 3 at longer aggregation times is not easy to explain. For example, what are the origins of the second plateau in the data at low q? Plots of the type seen in Fig. 3 may be explained in one of two ways: (1) the scattering function arises from a fractal-in-fractal type behaviour, i.e. larger secondary aggregates are mass fractal in nature and are constructed from the smaller primary aggregates that are themselves mass fractals; (2) the larger aggregates are of such a size that they give rise to a Fraunhofer diffraction pattern [23]. Using these two models it is possible to generate predicted scattering data from simple theory. Full details of these models will be published elsewhere and only the relevant results will be given here.

Examples of the predicted scattering intensity data for the two models, using relevant size information, are shown in Figs. 5 and 6. Also shown in Figs. 5 and 6 are the data for the t=30 min case from Fig. 3. For the fractal-in-fractal case, the lower limit of the length scale for the fractal behaviour in the primary aggregates is the size of the primary particles, whilst for the larger secondary aggregates, the lower limit of fractal length scale is the size of the primary aggregates. The upper limits are, of course, given by the primary and secondary aggregate sizes, respectively. Using these limiting sizes, a simple mathematical model can be generated. The results of such a fractal-in-fractal calculation are shown in Fig. 5. Clearly, these data do not readily fit the observed scattering from the real system.

In the second case, we can again use a simple fractal model for the primary aggregate scattering; in this case however, we add to it a scattering function calculated by assuming Fraunhofer diffraction from the secondary aggregates. The results of the fitting procedure are shown in Fig. 6. This time there is a remarkably good correlation between the predicted and actual data sets.

Further detail for Fraunhofer diffraction type scattering from large objects was obtained by measuring the scattered intensity as a function of scattering angle for non-flocculated glass spheres in water. Representative data of $\log I(q)$ against $\log q$ for four different sized sphere samples are shown in Fig. 7. Clearly, the scattering functions can be well modelled by, the simple Fraunhofer functional form used to generate

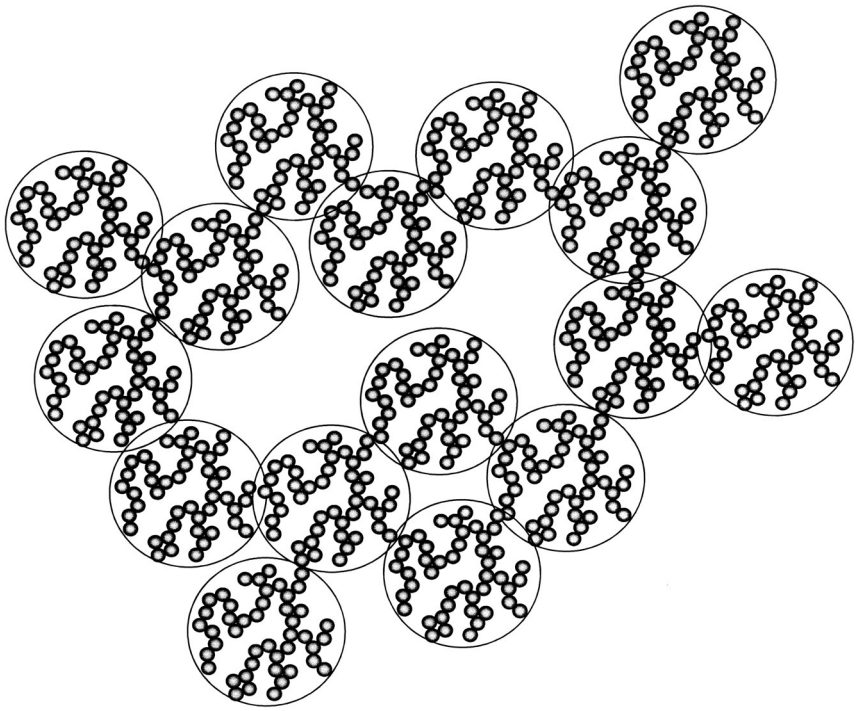

Fig. 4. A schematic representation of the structure of a fractal-in-fractal type aggregate.

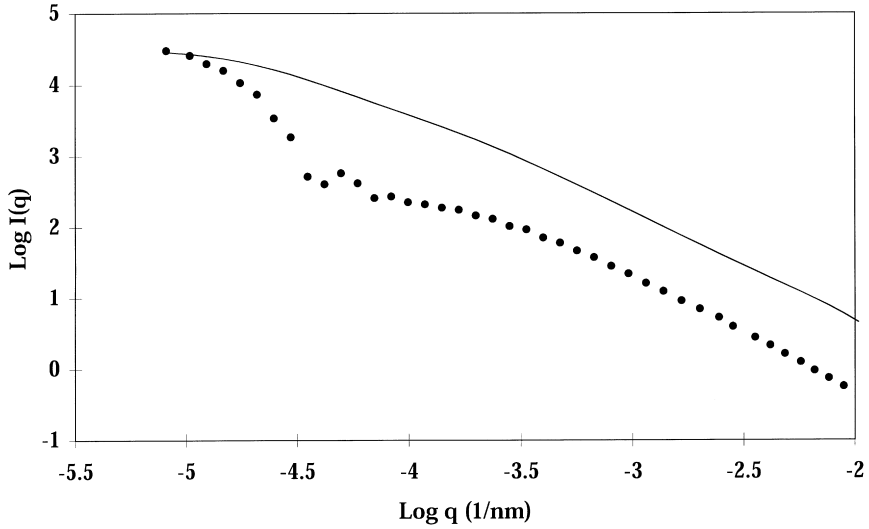

Fig. 5. Calculated scattering intensity as a function of q for a fractal-in-fractal model. Full line: calculated intensity determined using a primary particle radius of 165 nm, a primary aggregate radius of 13 μm, and a secondary aggregate radius of 100 μm. The fractal dimensions used in the calculation were 1.64 and 1.75 for the primary and secondary aggregates, respectively. Data points: t=30 min data from Fig. 3.

the data seen in Fig. 6. Note that the glass sphere samples are somewhat polydisperse in character; this has the effect of smoothing out the minima at larger q in the Fraunhofer diffraction pattern. It is worthwhile noting that we observe this type of scattering at all the single particle sizes measured down to a diameter of 5 μm; however, for the primary aggregates no scattering of this type is seen. The reason that this is not seen must be a combination of the tenuous nature and the relatively small sizes of the primary aggregates. A cursory examination of the data shown in Fig. 7 shows an apparently linear region in the $\log I(q)$ versus $\log q$ plots for $-3<\log q<-2$. This is the standard region used to determine fractal information. Indeed, if we determine the magnitude of the slope for the region corresponding to the 100–150 μm sample we obtain a value of 0.6. In terms of a fractal aggregate structure this value is meaningless. The form of the data in the region $-4<\log q<-2$ is as expected for an object which scatters light according to the Fraunhofer diffraction model; it is entirely different to the form of the data given in Fig. 3. Of course, in the case of isolated spheres there should be no fractal information available. It is possible that the Fraunhofer diffraction can alter the slope of the fractal region. In the data shown in Fig. 3, the effect of this would appear to be minimal. If we consider the model prediction shown in Fig. 6 then the intensity of the Fraunhofer component is too small in the relevant q range

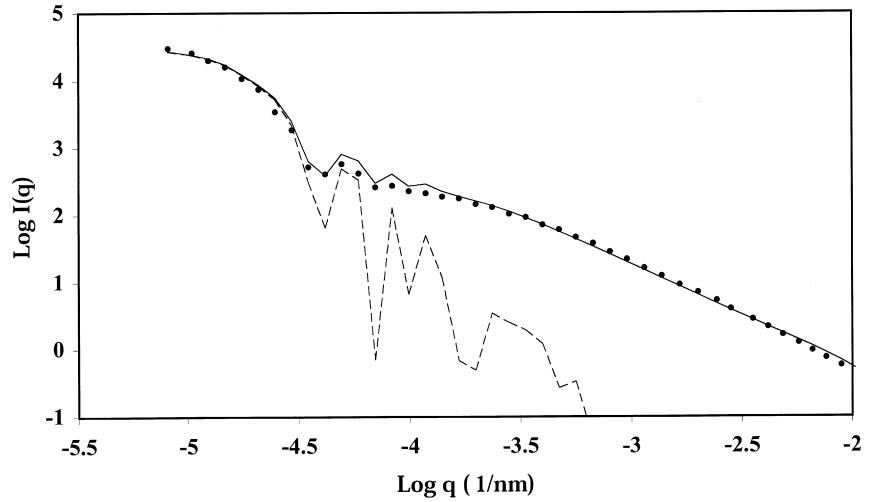

Fig. 6. Calculated scattering intensity as a function of q for a fractal plus Fraunhofer model. Full line: calculated intensity determined using a primary particle radius of 165 nm, a primary aggregate radius of 13 μm, and a secondary aggregate radius of 100 μm. Data points: t=30 min data from Fig. 3. Broken line: the Fraunhofer diffraction calculated from the large secondary aggregates.

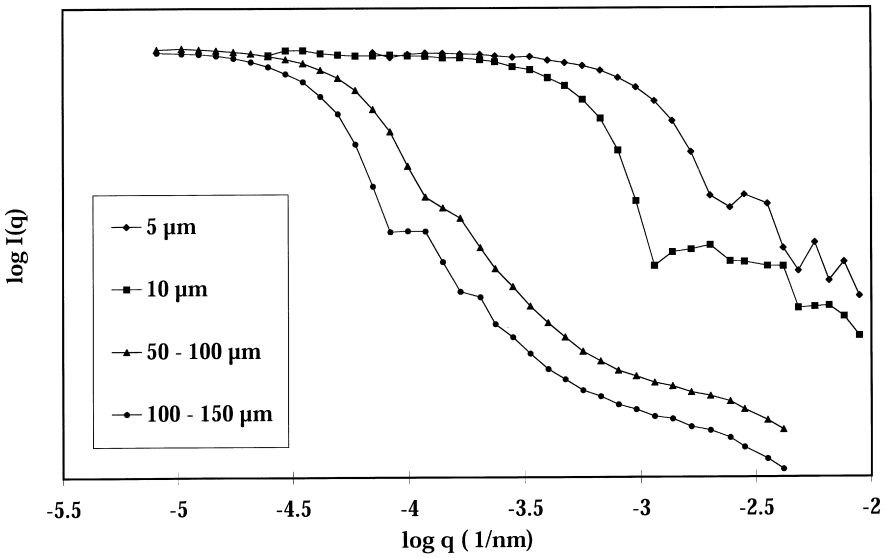

Fig. 7. The measured intensity of scattered light as a function of q collected for four different particle samples. The samples used were glass microbeads having the diameters shown. The data are presented on a double logarithmic scale. Note: The data sets have all been normalised to the same initial intensity at low q for ease of comparison.

to have any effect on the scattered intensity for the primary aggregates.

What are the consequences of these results? If we consider our predicted structure shown in Fig. 4 we are expecting a fractal-in-fractal structure. The aggregates in this system may well have this structure; however, we are unable to use low angle light scattering to probe the fractal characteristics of the secondary aggregates. The persistence of the scattering from the primary aggregates throughout the aggregation process suggests that the secondary aggregate structures are of a low density. If not, we would expect an increase in shadowing effects. This would result in a decrease in the intensity of scattering from these primary aggregates.

If we assume that the fractal scattering from the primary aggregates persists throughout the aggregation process then we can calculate the mass fractal dimensions for these units as a function of time. The data so obtained show an essentially invariant value of d_F, where $d_F = 1.64 \pm 0.05$; this again reinforces the idea that these structures are maintained throughout the aggregation. This number is at the low end of the scale for typical mass fractal dimensions from diffusion limited cluster–cluster aggregation [20]. It indicates a diffusion limited process with no subsequent structural rearrangements.

Further information about the bridging flocculation can be obtained from an investigation of the aggregate sizes as

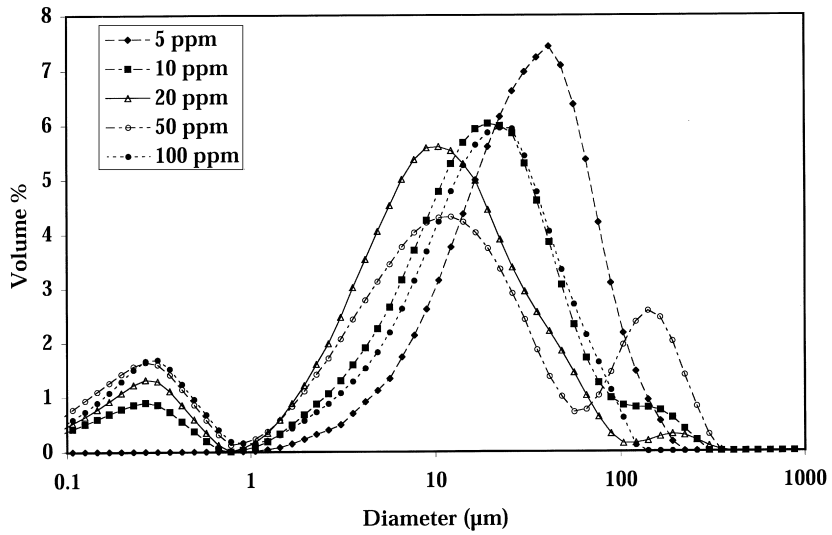

Fig. 8. Aggregate size distribution data as a function of added polymer concentration at a time t=2 min after mixing. The initial system conditions used (prior to dilution): particle concentration=0.05% (w/w); pH 6; (KNO_3)=10^{-4} M; T=25°C.

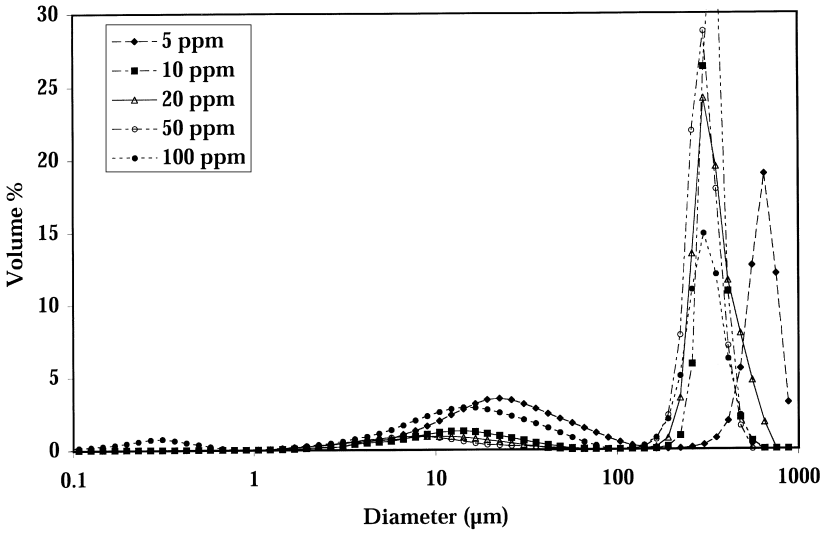

Fig. 9. Aggregate size distribution data as a function of added polymer concentration at a time t=30 mins after mixing. The initial system conditions used (prior to dilution): particle concentration=0.05% (w/w); pH 6; (KNO_3)=10^{-4} M; T=25°C.

a function of added polymer concentration. Data for the aggregate size distributions recorded at the initial and final times, for the polymer used here, at five added polymer concentrations are shown in Figs. 8 and 9. Examination of the number of primary particles still present immediately after cessation of stirring shows that their numbers increase as the copolymer concentration is increased. This is not surprising. As the polymer concentration increases, the rate of surface coverage by adsorbed polymer chains will also increase. At the lowest polymer concentration examined (5 ppm) no primary particles were seen at any time. Instead, we observe a substantial amount of the primary aggregates with a mean size of about 70 μm. In contrast, at 100 ppm polymer the initial data showed a substantial number of individual particles which did not completely disappear with time. Furthermore, the primary aggregates present had a smaller mean size of about 20 μm when compared to the 5 ppm case.

These effects are all easily explained from a consideration of the surface coverage by the polymer. Using the Healy and La Mer [5] optimum flocculation condition, the relatively large amount of primary particles observed at 100 ppm and their persistence with time suggests that the particles were well covered in this case with a polymer layer. At 5 ppm the complete absence of any primary particles indicates that bridging flocculation is efficient. In bridging flocculation with a high molecular weight polymer, it is typical to choose the polymer such that it has charged groups of a different sign than the particle surface. In this way, there will be a strong electrostatic interaction between groups along the polymer chain and the particles [6]. By choosing a high molecular weight, the polymer will occupy a large volume in the solution and may be able to interact with more than one particle [8].

As we discussed above, even at 5 ppm flocculant the current system is expected to be overdosed. However, the light scattering indicates that this does not stop flocculation.

The dynamic aspects of the flocculation process will be important for the systems examined here. On increasing our polymer concentration from 5 to 100 ppm we are increasing the number of polymer chains per particle (at 0.05% w/w) from about 8 to 160. If we assume a radius of gyration of around 60 nm for the polymer, and taking the particle radius as 165 nm, we calculate that if the polymer were to retain its solution conformation at the interface it would take approximately 30 chains to coat a single particle. Obviously, as discussed above, any chain that adsorbs to a surface will be expected to relax its conformation down towards that surface thereby maximising the favourable (in this case) surface-polymer contacts. However, if the particle collision rate is faster than the polymer adsorption rate, which is itself faster than the relaxation rate, then bridging flocculation could still occur. Under such conditions, as the particles become initially coated with some polymer they are continually colliding thereby facilitating aggregation. Furthermore, at 5 ppm polymer, initial adsorption with no polymer relaxation would be insufficient to completely coat the particle surface area. Of course, relaxation over time would allow even a single chain to fully coat one particle in the system studied here. However, again it is unlikely that this will occur due to the dynamic nature of the process. The fact that we see significant flocculation even at 100 ppm supports the above idea that the polymer adsorption and relaxation rates are slow compared to the particle collision rates.

The growth of the secondary size peaks under the perikinetic conditions over long time periods is easily understood. The results suggest that bridging flocs formed initially are size limited by the shear field they experience. When this

is removed they can aggregate further. Evidence that this aggregation is through a bridging process is compelling. The flocs formed are very strong and the rate of their formation is quickest at a lower polymer concentration; both effects are characteristic of bridging flocculation as described above.

The results presented here show clearly that light scattering techniques can be employed as a tool to generate some useful information about aggregate structures formed via a bridging flocculation mechanism.

5. Conclusions

In this paper, we present light scattering data collected from aggregates formed with a bridging flocculation mechanism. The data indicate clearly that the aggregation seen here, under the conditions used, is a two-stage process. This results in a primary aggregate structure that can be analysed for its mass fractal dimensions using a conventional approach. The mean radii of the aggregates formed in the first step typically are between 5 and 20 μm. The mass fractal dimension of these aggregates is $d_F = 1.64 \pm 0.05$. A second aggregation step then follows in which the primary aggregates flocculate together forming much larger secondary aggregates. The structure of these aggregates cannot be determined from light scattering data using standard fractal analyses. The mean radii of the secondary aggregates are between 100 and 400 μm. Evidence that the secondary aggregates are formed from aggregation of the primary aggregates is also obtained from data for the scattered intensity as a function of scattering angle. As a function of aggregation time, the scattered intensity from the primary aggregates was seen to be invariant despite the fact that they were observed to ‘disappear’ from the size distribution data. This can only be explained if they are still present within the secondary structures.

Acknowledgements

The authors recognise the support of the Centre for Multiphase Processes, a Special Research Centre of the Australian Research Council.

References

[1] Y. Otsubo, Heterogeneous Chem. Rev. 3 (1996) 327.
[2] R.A. Ruehrwein, D.W. Ward, Soil Sci. 73 (1952) 485.
[3] V.K. La Mer, Discuss. Faraday 42 (1966) 248.
[4] R.H. Smellie, V.K. La Mer, J. Colloid Sci. 23 (1958) 589.
[5] T.W. Healy, V.K. La Mer, J. Colloid Sci. 19 (1964) 323.
[6] M. Elimelich, J. Gregory, X. Jia, R. Williams, Particle Deposition and Aggregation: Measurement, Modelling and Simulation, Butterworth-Heinemann, Oxford, 1995.
[7] J. Gregory, Colloids, Surf. 31 (1988) 231
[8] S.F. Sun, Physical Chemistry of Macromolecules: Basic Principles and Issues (1994) Wiley-InterscienceNew York.
[9] X. Yu, P. Somasundaran, J. Colloid Interface Sci. 177 (1996) 283.
[10] M.A. Cohen-Stuart, G. Fleer, Ann. Rev. Mater. Sci. 26 (1996) 463.
[11] Y. Adachi, M.A. Cohen-Stuart, R. Fokkink, J. Colloid Interface Sci. 167 (1994) 346.
[12] R. Hogg, J. Colloid Interface Sci. 102 (1984) 232.
[13] J-P. Hsu, D-P. Lin, Colloid Polym. Sci. 274 (1996) 172.
[14] Y. Otsubo, K. Watanabe, J. Colloid Interface Sci. 122 (1988) 346.
[15] J. Buffle, G.G. Leppard, Environ. Sci. Technol. 29 (1995) 2169.
[16] D. Perret, M. Newman, J.C. Negre, Y. Chen, J. Buffle, Water Res. 28 (1994) 107.
[17] S. Stoll, J. Buffle, J. Colloid Interface Sci. 180 (1996) 548.
[18] S. Stoll, J. Buffle, J. Colloid Interface Sci. 205 (1998) 290.
[19] M.Y. Lin, H.M. Lindsay, D.A. Weitz, R.C. Ball, R. Klein, P. Meakin, Phys. Rev. A 41 (1990) 2005.
[20] M.Y. Lin, H.M. Lindsay, D.A. Weitz, R.C. Ball, R. Klein, P. Meakin, J. Phys: Condens. Matter 2 (1990) 3093.
[21] J. Teixeira, J. Appl. Cryst. 21 (1988) 781.
[22] J.W Goodwin, J. Hearn, C.C. Ho, R.H. Ottewill, Colloid Polym. Sci. 252 (1974) 464.
[23] H.C. van de Hulst, Light Scattering by Small Particles (1981) Dover Publications, New York